Frequency, intensity, and duration of thermal inversions in the Jura Mountains of France

Daniel Joly, Yves Richard

Frequency, intensity, and duration of thermal inversions in the Jura Mountains of France

JOLY D.[1], RICHARD Y.[2]

[1] *Laboratoire ThéMA, CNRS and Université Bourgogne Franche-Comté, Besançon*
E-mail: daniel.joly@univ-fcomte.fr; tel.: +33 3 81 66 54 02 ; ORCHID: 0000-0002-4817-1779
[2] *Centre de Recherches de Climatologie / Biogéosciences, CNRS and Université Bourgogne Franche-Comté, Dijon; Yves.richard@u-bourgogne.fr*

Abstract

This analysis of the frequency, intensity, and duration of thermal inversions is based on daily minimum (tn) and maximum (tx) temperatures recorded over three years at 16 pairs of data loggers located under forest cover in the Jura Mountains of France. Each pair consists of a logger located at the bottom of a depression and another located higher up either nearby (local site) or more than 40 km away (regional site). The daily frequency of inversions is maximum at local sites for tn (50%) and minimum for tx at regional sites (4%). The maximum intensity of the inversions reaches 15.1 °C for tn and 16.2 °C for tx. The average intensity is about 2 °C: 1.5 °C for tx at local sites and 2.4 °C at regional sites. The duration of inversions is generally short: 60% of them last less than a day. Of the inversions that last for more than one day, 15% exceed 3 days and the maximum duration observed is 22 days. The relationship between the diurnal amplitude of temperature and the frequency, intensity, and duration of inversions indicates that mesoscale atmospheric conditions directly influence inversions.

Key words: temperature, inversion, altitudinal lapse rate, forest.

1 Introduction

Temperature inversions are a weather phenomenon that has been known for a very long time (e.g. Marvin, 1914). But interest in their study has intensified in recent decades because they are associated with peaks of pollution (Kukkonen et al., 2005; El Melki, 2007; Ji et al., 2012; Lareau et al., 2013; Chemel et al., 2016; Largeron and Staquet, 2016; Paci et al., 2016; Czarnecka and Nidzgorska-Lencewicz, 2017; Zhang et al., 2017). However, researchers' attention to this phenomenon is not limited to pollution. Other works consider the effects of inversions on vegetation (Blennow and Lindkvist, 2000; Dobrowski, 2011; Hannah et al., 2014; Schuster et al., 2014; Shimokawabe et al., 2015; Patsiou et al., 2017) or on the mass balance of glaciers (Mernild and Liston, 2009).

There are many types of thermal inversions (Barry, 2008) classified by the mechanisms that generate them: subsidence inversions, advective inversions, contact inversions, and radiative inversions (Busch et al., 1982). Subsidence inversions occur most often within the tropical belt, but also, however rarely, in other climate zones (Mirocha and Branko, 2010; Dupont et al., 2016; Mo et al., 2014). They occur at high altitudes by adiabatic compression of the air inside a high pressure system. Advective inversions can extend over large areas and occur when warm air slides over the cold boundary layer (Streten et al. 1974; Oke 1987; Milionis and Davies, 2008; Mernild and Liston, 2009). Contact inversions occur when a surface of ice or cold water cools the air that comes into contact with it (Sotiropoulou et al., 2016). They mainly affect the Arctic zone (Kadygrov et al., 2005) where they are frequently more than 1.5 km thick and last almost all year round over the ice pack (Barry, 1983).

Radiation inversions, due to the radiative deficit at the ground surface, are most frequent in the temperate zone. In general, in mid-afternoon, the temperature at the ground surface and in the very low layers of the atmosphere is warmer than in the higher layers. When the surface begins to receive less energy than it emits the earth/atmosphere radiation balance becomes unfavorable for the surface and its temperature falls. If this process continues long enough, there comes a time when a state of equilibrium is reached. Then, if it continues, the balance becomes negative and the surface temperature falls below that of the overlying atmosphere: there is thermal inversion. These radiative or nocturnal inversions (Barry, 2008) occur most often when skies are calm and clear. Such inversions often dissipate in the early morning (Anquetin et al., 1998) but, if weather conditions allow, they may persist for several days. (Vitasse, 2017). This inversion phenomenon is intensified by the local topography: cold air flows

downslope and accumulates at the bottom of the topographic lows (Papadopoulos and Helmis, 1999; Mahrt et al., 2010; Fernando et al., 2013) in such a way that the cool-air pools (CAPs) that develop in such contexts are totally decoupled from the overlying synoptic flow (Daly et al., 2010; Largeron and Staquet, 2016).

The altitude of the surface layer that marks the vertical extension of the inversion is attributed to the combined effects of topography (spatial factors) and synoptic conditions (time factors) (Kahl, 1990; Mahrt and Heald, 2015; Dorninger et al., 2011). It rarely exceeds 200 m above a flat surface but is thicker above a topographic basin where cold air accumulates (Largeron and Staquet, 2016). Surface characteristics play a major role: inversions are very frequent in winter when the snow-covered ground increases radiative cooling and prevents surface warming. The presence of forest also plays a role in the formation of the boundary layer (Kiefer and Zhong, 2015).

Inversions are most often observed using two approaches: the first is to observe the stratification of air in the open atmosphere above the surface; the second is to compare temperature measurements taken at two or more separate sites just above the ground surface. The most commonly used method in the first case is radio sounding (Pepin and Duane, 2007; Antonioli, 2016; Guédjé et al., 2017) whose measurements, made from the ground to altitudes of up to 50 km, are recorded on emagrams. The mast along which several sensors are positioned is a way of observing the stratification of the air near the ground (Brümmer and Schultze, 2015). Another increasingly common process is the use of affordable angular scanning microwave temperature profile radiometers for the long-term monitoring of temperature profiles at high vertical and temporal resolutions (Wolf et al., 2016). But these various means are costly and technically difficult to implement. An advantageous alternative is to use the existing network of weather stations (Fallot, 2012; Kirchner et al., 2013) or, if there are insufficient stations, to create a new autonomous measurement network (Vitasse et al., 2017). It should be noted that the two modes of observation of inversions do not provide exactly the same frequency and intensity values (Pepin and Norris, 2005).

The objective of this study is to analyze the frequency, intensity, and duration of inversions observed in the Jura Mountains of France. Temperature data were recorded over three years using an original network of data logger deployed under forest cover (UFC). We use the daily minimum (tn) and maximum (tx) temperatures from 16 pairs of loggers. Each pair consists of one logger located at the bottom of the depression and a second located on a ridge or on high slopes. The two are separated by a large enough difference in altitude to reveal significant temperature differences. By using the network of Météo-France, UFC inversions can be compared with open-site (OS) inversions. Finally, the analysis is made at two scales: local inversions for which loggers are located close together and regional inversions for which loggers are more than 40 km apart.

2 Material and method

The study area is on the French side of the Jura Mountains. It is characterized by a temperate oceanic climate with a continental tendency that is strongly influenced by the presence of medium-altitude mountains (Figure 1). It is bordered to the north by the Doubs valley, to the east and south by the Jura ridges. The three topographical units of the Jura Mountains of France are represented, with, from west to east, the plain (200, 250 m), the two plateaus (300–600m), and the Haute-Chaîne that rises to 1300 m.

Figure 1. Study area and location of measurement points: data loggers UFC (Under Forest Canopy) and stations OS (Météo-France open sites). Points in the lower position are designated by a letter with no number. The La Brévine data loggers network (Vitasse et al., 2017) in Switzerland is shown on the map because it is referred to several times in this contribution

2.1 Data

A network of 48 UFC temperature stations instrumented with a data logger has been in operation since the end of 2014. Twenty-five loggers were first located so that they could be paired with one of the "open site" weather stations in the Météo-France (MF) network. Because the MF weather stations are located in flat topographical settings, the others sample certain specific sites omitted by the MF stations,

for example the sides or bottoms of deep valleys. This spatial distribution of the stations provides good conditions for studying thermal inversions.

The UFC network has eight loggers located at the bottom of topographic depressions (valleys, synclines): these are the low loggers in our set-up. These low loggers are paired with loggers located at an altitude at least 50 m higher. Distance is taken into account for pairings. First, they are paired with the nearest logger(s) within a 20 km radius. In these cases, the pairs are used to track local inversions (Figure 1). As two of the eight loggers in low positions are connected to more than one high logger, 12 local pairs are composed. Three pairs are located in the lower-lying land, one is located on the plateau (F-F1), and the other eight are located in the mountains. The average distance between the loggers making up each local pair is 8.5 km and the average altitudinal amplitude 250 m. Second, loggers located more than 20 km apart are paired. These regional pairs are based on the three low loggers located around the Jura arc at an altitude of less than 330 m (A, B, and C in Figure 1) combined with the four high loggers that punctuate the ridges of the Jura between 981 and 1235 m above sea level. The average distance between the loggers of each regional pair is 58 km and the average altitudinal amplitude 830 m.

Temperatures were measured by each logger every 6 minutes using HOBO PRO V type sensors fitted in protective cases fastened to the north side of trees at 2 m above ground level (Joly, 2015). The recordings ran for three full years from 1 January 2015 to 31 December 2017, with 5.2% of the data missing. The daily minimum and maximum readings were extracted from the database.

UFC temperatures differ significantly from temperatures measured at nearby open sites (Joly, 2015; Gaudio et al., 2017). It is possible therefore to imagine that the characters of the inversions detected there are also different. Measurements show that air temperature differences between open areas and UFC areas, which are in the order of 1 to 2 °C near the ground, decrease with height and are less than 1 °C at a height of 40 m (Karlsson, 2000; Kiefer and Zhong S., 2015). Under these conditions, the inversion extends well above the forest cover. To test the influence of forest cover on inversions, the characteristics of pairs of UFC ls are compared to those of pairs of MF stations located in open sites (Figure 1), each pair being located just a short distance from the other. Of the 30 MF stations available, only 10 (five pairs) meet the location criteria defined above: three (Amf-A2, Cmf-C2 and Emf-E2) concern local inversions and two (Amf-A4 and Bmf-E2) regional inversions.

In this paper, the terms "sensor", "station" and "logger" refer respectively to (1) the device used to measure temperature, (2) the measurement points managed by the official institutions accredited by the WMO and (3) the elements of the network under forest cover that we have set up in the Jura.

2.2 Method

The delta between the two loggers of each pair (high logger temperature - low logger temperature) is calculated separately for daily tn and tx. A negative result is obtained for a “normal” altitudinal decrease in temperatures. A positive result indicates a thermal inversion. Three indicators (frequency, intensity, and duration) are calculated to characterize the inversions. Calculations are made according to two time steps for the three years: daily (1096 days in all) and monthly (36 months).

The tn and tx of the stations managed by MF closest to each site are used to calculate the daily thermal amplitude, an excellent proxy for atmospheric conditions that are highly correlated to inversion characteristics (Dorninger et al., 2011; Vitasse et al., 2017). The diurnal amplitude of temperature provides information on the amount of solar radiation received or on cloud cover (Erpicum, 2004). The daily thermal amplitudes also depend on the season. As a general rule, the highest amplitudes are observed during summer when the radiative effects are most marked. To reduce this effect, the year is segmented into four seasons: winter (December, January, February), spring (March, April, May), summer (June, July, August), and fall (September, October, November).

3 Results

3.1 Sensitivity of inversions to space and time factors

3.1.1 Site sensitivity: under forest cover versus open site

The frequency of UFC inversions is similar to that detected in open environments with one exception: the frequency of local inversions for tx UFC (25.9%) is twice as high as that of open sites (Table 1). This difference can be largely attributed to the UFC site A-A1 whose very high inversion frequency during tx (45.9%) pulls the average upwards. This single anomaly does not invalidate our results, especially since the nearby OS site (Amf-A2) show similar inversion frequencies. The intensity of inversions is slightly higher in open sites than under forest cover while the duration of the inversion sequences is similar in both settings.

When significant differences appear, they are sporadic and, since the number of logger pairs is small, their impact on averages is high. The results of our study of UFC inversions can therefore be considered as closely reflecting the characteristics of open site inversions. This observation is in line with the conclusion of an earlier study that revealed that spatial variation in temperature under forest cover and in open areas is controlled by the same topographic factors (Joly and Gillet, 2017).

Table 1. Frequency and intensity of inversions, duration of inversion sequences under forest cover (UFC) and in Météo-France open sites (OS)

	tn-UFC	tn-OS	tx-UFC	tx-OS
Local frequency (%)	36.1	37.4	25.9	11.6
Regional frequency (%)	7.1	5.5	4.0	6.7
Local intensity (°C)	12.7	19.2	15.1	19.5
Regional intensity (°C)	14.5	14.6	26	30.7
	Local-UFC	Local-OS	Reg.-UFC	Reg-OS
Duration (day)	1.9	1.7	1.6	1.8

3.1.2 Site sensitivity: local versus regional

Figure 2. Night temperature deltas (tn) by scale, pair, and day.
High: local scale, low: regional scale. Each row represents a pair and each column represents a day. Blank: missing values

Some pairings are not conducive to the development of nocturnal inversions: for example, DD4 for the local scale and AA3 for the regional scale. Others, on the contrary, cause frequent and marked inversions: for example, DD3 for the local scale and BG2 for the regional scale (Figure 2). But this figure above all makes it possible to observe the simultaneity of nocturnal inversions (tn) according to the pair or to the scale (local or regional). Overall, this simultaneity is respected and indicates that the different pairings are representative of relatively widespread inversion situations on both of the scales considered.

3.1.3 Sensitivity to time sample: three years

Since the sample is relatively short (three years), the frequency, intensity, and duration of inversions are calculated year by year. The objective is to test the sensitivity of the three indices developed to characterize thermal inversions with respect to weather conditions that may vary from one year to the next. Interannual frequency variations are not high: 57% in 2015, 48% in 2016, and 55% in 2017. For intensities, there is also little variation from one year to another: the average intensity of inversions during the three years of observation is between 2.0 °C and 2.3 °C for tn and between 1.6 °C and 1.8 °C for tx. The durations are remarkably stable from one year to the next: between 2.1 and 2.2 days on

average for local inversions and between 1.1 and 1.3 days for regional inversions. Sensitivity to temporal sampling (three years) is low and allows conclusions to be drawn that are likely to be generalizable.

3.2 Frequency, intensity, and duration of inversions at the annual scale

Table 2 clearly shows that nocturnal inversions (tn) are far more frequent than diurnal inversions (tx) and that local inversions are more frequent than regional inversions.

Table 2. Average frequency, intensity, and duration of inversions during tn and tx.

	Local-tn	Local-tx	Regional-tn	Regional-tx
Frequency (%)	52.6	20.1	13.6	4.2
Intensity (°C)	2.1	1.5	1.9	2.4
	Local		Regional	
Duration (days)	2.2		1.5	

Over the three years of observation and for the 12 local pairings, local inversions occur on average 52.6% for tn and 20.1% for tx (Table 2; Figure 3). Regional inversions are much less frequent. The quartiles of regional inversions have values about 40% lower than those of local inversions: the difference between the extreme values of local and regional inversions is half as wide (Figure 4).

The minimum intensity of thermal inversions is, because of the way inversions are calculated, just above zero (0.1 °C) for both tn and tx (Figure 4). The maximum intensity (15.1 °C and 16.2 °C for tn and tx) is very much higher than all quartiles, reflecting the exceptional nature of the powerful inversions. In fact, only 8 and 6% of the tn and tx inversions are of more than 5 °C, and less than 1% exceed 10 °C. For tn, the average inversion is stronger at the local than regional level, while for tx the highest average intensity is observed at the regional level. Similarly, it is difficult to indicate which of the two times of the day, night tn or day tx, gives rise to the strongest inversions (Table 2). Thus, the intensity of inversions is more complex to analyze than their frequency.

Finally, according to our observations, the duration of local inversions is longer than that of regional inversions (Table 2). The minimum duration of an inversion can be short when a tn with inversion is surrounded by two tx without inversions or when a tx with inversion is surrounded by two tn without inversions. But, depending on the persistence of the conditions that caused it and the topography of the sites, the inversion may last longer: several days or even weeks. We call “sequence” any set of n successive days of inversion at a given site.

Figure 3: Frequency of local (loc) and regional (reg) inversions for tn and tx

Local inversions that affect the tn and then disappear during the day are observed on average every third day (31.7%); those that affect the tx only are much rarer: 2.5%. Ephemeral regional inversions affect on average 10.1% of tn and 1.9% of tx. The average number of local inversion sequences (793) is 12 times higher than the average number of regional inversion sequences (64). The average duration of local and regional inversion sequences is 2.2 and 1.5 days. These short average durations are explained by the predominance of short sequences of 1 to 3 days, 85% and 94% of which are for local and regional inversions respectively (Table 3). Sequences of 10 days or more are rare (7% and 2%) but they may last for a long time (maximum: 22 days, site F-F1 from 10 December to 31 December 2015).

Table 3. Proportion of the duration of local and regional inversion sequences (days) distributed into six value classes

	1	2	3	4-5	6-10	> 10

local (%)	55.7	20.9	8.4	7.4	5.8	1.6
Régional (%)	76.6	12.5	4.7	4.7	1.6	

Figure 4 provides an analysis of all distributions. Intensity and duration of local inversions are characterized by particularly asymmetric distributions. Thus, the averages calculated for these quantities are very sensitive to a few rare outliers and must be analyzed with caution. Frequency averages, with less asymmetric distributions, are more robust than averages calculated for intensities and durations.

Figure 4: Box plot of frequencies (4 pairings are considered for regional inversions [v1, ..., v4], frequency value is done for each of the 4 inversions), intensities (9295 and 338 local inversions for tn, tx), and durations (1275 inversion sequences)

3.3 Frequency, intensity, and duration of inversions at the seasonal scale

Inversions are most frequent in winter (Figure 5A). Only for local night inversions do summer frequencies tend to be comparable to those of December (65%). Values for late winter and spring are less than or equal to 50%. It is noteworthy that, during the December tn, three pairings (F-F1, G-G1, and H-H1), all in the east of the study area, have inversion frequencies greater than 80%.

The winter months (DJF) are different from the rest of the year with high intensities in all configurations. The variation in inversion intensity is fairly stable from spring to fall in all cases (Figure 5B). The seasonal variation in the duration of local inversions (Figure 5C) contrasts spring with short inversions (1.5 days) with fall and winter, seasons during which inversions occur on average 2.5 to 3 days. Regional inversion sequences last on average one day during those months in which they are observed except December (1.6 days).

Figure 5: Average monthly (A) frequency, (B) intensity, and (C) duration of local and regional inversions for tn and tx

3.4 Mesoscale Weather conditions associated with inversions

Most works on temperature inversions mention that their characteristics are very sensitive to the mesoscale weather. We found it interesting to look at how frequency, intensity, and duration of inversions vary according to the diurnal amplitude of temperature, which is an indicator of calm and radiative (high amplitude) or covered and disturbed (low amplitude) atmospheric conditions. In detail, each diurnal temperature amplitude value is associated with a large number of situations that have varying occurrences, intensities, and inversion times over the study area. This diversity produces statistical noise that is detrimental to the identification of the major trends that link these two variables. To reduce this instability, the average frequencies and intensities were calculated as part of classes grouping amplitude values by whole units. This operation produces 23 statistical individuals characterized by an amplitude class (class 1 = 0 to 0.9 °C, class 2 = 1 to 1.9 °C, …, class 23 = 22 to 26.1 °C) and an average frequency, intensity, and duration of inversion.

3.4.1 Diurnal amplitude of temperature and frequency of inversions

A positive linear relationship is observed between the diurnal amplitude of temperature and the frequency of nocturnal inversions (tn) (Figure 6A). But, the relationship between these two variables is not clearly marked for daytime inversions (tx).

Figure 6: Daily thermal amplitude versus (A) frequency and (B) intensity of local (loc) and regional (reg) inversions for tn and tx

At the end of the night (tn), the relationship between diurnal temperature amplitude and inversion frequency is observed at all seasons for local sites (Figure 7A). The frequency of local tn inversions (W-

loc) is highest in winter up to the diurnal amplitude of 18 °C where a maximum (95%) is reached. In summer (S-loc), the relationship between diurnal temperature amplitude and inversion frequency is slightly lower but almost linear. For regional sites, the relationship between tn inversion frequency and diurnal temperature amplitude is observed in winter from the amplitude value of 6 °C and in summer from 15 °C amplitude.

Figure 7: Variation of daily thermal amplitude vs frequency of local (loc) and regional (reg) inversions in winter (W) and summer (S) during tn (A) and tx (B). Legend common to both graphs

For tx, the relationship between diurnal amplitude of temperature and inversion frequency (W-loc in Figure 7B) is quite sensitive in winter for local sites up to 13 °C and for regional sites (W-reg) from 10 °C. In summer, the diurnal amplitude of temperature seems to have no influence on the frequency of local and regional inversions.

3.4.2 Diurnal amplitude of temperature and inversion intensity

The correlation between the 23 classes of diurnal amplitude of temperature vs the intensity of inversions produces results similar to those just described for frequency (Figure 6B). The average intensity of nocturnal inversions (tn) increases as the daily temperature amplitude increases (Figure 8A). When the daily temperature amplitude is low (< 6 °C), the intensity of inversions is less than 0.3 °C. Conversely, when the thermal amplitude exceeds 17 °C, the intensity of inversions is greater than 4 °C in winter for local sites and 3 °C for regional sites. In summer, the values are lower (2 °C for local sites, 0.5 °C for regional sites).

During the daytime (tx), the average intensity per amplitude class is very low and there is almost no covariation with the diurnal amplitude of temperature: the increase in thermal amplitudes leads to a very moderate increase in the intensity of inversions in winter only and especially for local sites (Figure 8B).

Figure 8: Variation of the average daily temperature amplitude vs the intensity of local inversions during (A) tn and (B) tx for winter and summer

3.4.3 Diurnal amplitude of temperature and inversion duration

The diurnal amplitude has an appreciable influence on the average duration of inversions especially for tn and in winter. With local winter inversions, a plot of the relationship between diurnal amplitude of temperature and tn inversion duration forms an inverted parabola (Figure 9A). Low amplitudes (<3 °C) lead to short inversions (< 0.35 days on average), then an increase in the amplitude to 12 °C leads to an increase in the duration of inversions, which reach a ceiling (0.5 days on average). Further increase in diurnal amplitude results in a sharp drop in the duration of the inversions to such an extent that, beyond a daytime amplitude of 21 °C, inversions sequences are non-existent (0 days on average). The local inversions of the other seasons exhibit similar behavior with two differences: duration is half as long and the phases of increase and decrease of duration as a function of the daytime amplitudes are asymmetric.

With regional inversions (Figure 9B), the relationship between amplitude and duration in winter is identical to that for local inversions: increase in the length of duration up to 13 °C then shortening. Sequence inversions are almost non-existent in spring, summer, and fall.

Figure 9: Variation of daily thermal amplitude average (12 pairings) vs duration of (A) local and (B) regional inversions for the four seasons

4 Discussion

Several results will be discussed in the light of the work already done on inversion characters. First, it should be noted that the inversion characters depend on the choice of stations (Mahrt and Heald, 2015).

We will thus have to discuss the values of frequency, intensity, and duration of inversions revealed by our study insofar as we have from the outset chosen experimental conditions that favor the occurrence of inversions. Indeed, cold air slides down the slopes of topographic depressions and accumulates (Kirchner et al., 2013; Vitasse et al., 2017) reinforcing inversions. Our contribution confirms that the frequency of inversions depends on a large number of factors. This explains the great spatial and temporal variability of their occurrences. Second, it should be noted that frequency is the most widely described character of inversions, while statistics on the intensity and duration of inversions are poorly documented in the work we have consulted. Finally, because the relevant information is unavailable, we will not talk about snow, which several studies report as influencing inversions (Pepin and Norris, 2005; Kirchner et al., 2013; Foster et al., 2017; Vitasse et al., 2017). That said, the influence of snow on the characteristics of inversions is necessarily reflected in the statistics that contrast winter with the other seasons.

4.2 The characters of local inversions

4.2.1 Frequency

The frequency of inversions varies greatly depending on location and time. While inversion is widespread in the Arctic (Kahl 1990; Kadygrov et al., 2005), it is not so in temperate regions. In coastal locations, surface inversions are rare but inversions are much more frequent at an altitude of 200 m (Milionis and Davies, 2008) and their frequency increases as one sinks inland (Hosler, 1961). Inversions are more frequent in winter and fall (coastal zone = 30%, inland = 35%) than in summer (respectively 22%, and 25%).

In flat areas, inversions are most often detected by means of masts or radiosondes. The values differ depending on where the surveys are conducted. In Hamburg (Germany), a 7-year study shows that inversions occur 27% of the time, with surface-based inversions 15% and elevated inversions 12% of the time (Brümmer and Schultze, 2015). In the Po Valley in Italy, the frequency of inversions over a 3-year period is between 37% and 50%, with much higher values in winter (72%) than in spring and summer (29%) (Antonioli, 2016). In topographically complex areas, inversions are examined by means of temperature loggers placed 2 m above the ground surface. In the Spanish Pyrenees, an analysis (40 loggers, 2 years of measurements) of the frequency distribution of surface inversions according to time of day and season shows a maximum in winter (86%) and mornings (38%). However, there is still a significant proportion (38%) of inversions at noon and in the late afternoon in January and December (Pagès et al., 2017). In the Western European Alps, between 2003 and 2014, the percentage of inversions between a valley station and a slope station is 28.6% for tn and 16.6% for tx (Nigreli et al., 2017). The Brévine valley (Swiss Jura) very close to our study area (Figure 1) was studied in winter (December 2014–February 2015) using 44 loggers. Inversions are observed on 43% of winter nights (Vitasse et al., 2017).

The values we obtained in the Jura (frequency of 53% during tn and 20% during tx) are in line with the average of the values returned by all the above-mentioned works related to temperature loggers placed 2 m above the ground surface. December is also the month when local inversions are most frequent (67% during tn, 50% during tx). However, it should be noted that our system is not optimal. Forests are rarely found at the bottom of valleys, which are primarily occupied by agriculture and built areas. Thus, in most of our study sites, the low loggers are located at the foot of the slope, a few tens of meters up from the valley floor. In this way, it is likely that a significant percentage of pellicular inversions are not captured. However, this remark must be relativized since, according to Largeron and Staquet (2016), cold air can fill the entire valley, especially during persistent inversions.

4.2.2 Intensity of inversions

Inversions may be characterized by the frequency with which certain intensity thresholds are exceeded. In a small area of low hills in the United Kingdom, Price et al. (2011) report the frequencies of inversion intensity threshold exceedances between the hilltop and two valleys as follows: strong inversions ≥ 4 °C recorded on 15% to 25% of nights depending on the valley considered and very strong inversions ≥ 6 °C on 3% to 6% of nights. The corresponding values for the average of our 12 sites in the Jura are comparable: 15.4% and 3.9% respectively. However, values much higher than those of Price et al.

(39.2% and 16.6% respectively for the strong and the very strong inversions) are obtained at site G (10 km from La Brévine) where the intensity of inversions is the highest of our 12 sites. In the small valley of La Brévine, Vitasse et al. (2017) note that the maximum intensity is 28 °C while the frequency of intensities above 10 °C is 77%. These values are much higher than those obtained in the Arve valley in the Alps (Paci et al., 2016) and at our site G where the maximum intensity is 15.1 °C (the frequency of intensities above 10 °C is only 4.3%).

4.2.3 Duration of inversions

The few studies that deal with the duration of inversions focus mainly on persistent cold-air pools (CAPs) to understand the processes (Whiteman et al, 1999, 2001; Price et al., 2011) or to better analyze the pollution episodes associated with them (the Passy-2015 field campaign in the Chamonix–Mont-Blanc Valley France: Paci et al., 2015). We have seen that the inversions that are destroyed during the day by thermal convection in the surface layer are the most numerous. Inversions that last at least three days (threshold used by Largeron and Staquet (2016) to define persistent inversions) account for 35–36% of inversion durations in alpine valleys (Largeron, Staquet, 2016) and in the Colorado Basin (Whiteman et al., 1999). In the current study, they represent 23.3% of the inversion sequences and the cumulative duration of the latter, expressed as a percentage of the total time (1096 days) is low (16.1%). However, to the east of the study area, where the continental influence is more pronounced than elsewhere, the cumulative duration of persistent inversions is longer (values of 45.7% for site H and 35.6% for site F, which is comparable to or even higher than figures for the two studies mentioned).

4.3 Influence of the frequency and intensity of inversions on the altitudinal temperature lapse rate

An important question addressed by topoclimatology is to explain why the altitudinal temperature lapse rate (ATLR) varies with location (Rolland, 2003; Gardner et al., 2009; Prömmel et al., 2010; Kirchner et al., 2013; Li et al., 2015; Nigreli et al., 2017; Joly et al., 2018). The main reason given by these researchers relates to the frequency and intensity of inversions. In our case, the ATLR is -0.31 °C/100 m for tn and -0.59 °C/100 m for tx. There is therefore convergence between these results and those of the inversion frequency which show higher values for tn than tx. The seasonal variation of the ATLR with lower values in winter than in summer (Rolland, 2003) is also consistent with our results, which show a higher frequency of inversions during the cold season, particularly in December.

Our loggers network allows us to quantify by correlation the relationship between the frequency and intensity of inversions and ATLR. To do this, we rely on the *36 average monthly* values of each of the *4 regional pairings*, the only ones to offer a sufficient altitudinal amplitude to calculate the ATLR. The average monthly frequency and intensity value (calculated for each of these 144 (36*4) statistical individuals) is also calculated to produce another indicator, *the inversion magnitude* (IM), which is a synthetic value obtained by multiplying the frequency (expressed from 0 to 1) by the intensity (expressed in °C). The IM values (°C) are between 0 (total absence of inversion for a full month) and, respectively for tn and tx, 3.7 °C (December 2016; site G-G2: frequency = 77% [converted to 0.77] and intensity = 4.8 °C) and 1.9 °C (December 2016; site C-H1: frequency = 55% [0.55] and intensity = 3.5 °C).

The correlation shows that IM explains 66% of the monthly variation in ATLR for tn but much less (43%) for tx (Figure 10). For tn, when the frequency and intensity of inversions are zero, ATLR is between -0.25 and -0.62 °C/100 m with an average of -0.48 °C/100 m. But, when IM increases, the gradient also increases, even exceeding 0 when IM > 2. For tx, ATLRs associated with no inversion are lower, ranging from -0.28 to -1 °C/100 m with an average of -0.65 °C/100 m. This very large dispersion of ATLRs is explained by regional climatology factors. For example, the abnormally high temperatures that occur in the upper logger at site A3 during the summer (due to its southerly position?) cause a high gradient (> -0.4 °C/100 m) between it and the lower logger (A) with which it is paired (temperatures of the upper logger repeatedly approach those of the lower logger). The very low ATLRs (around -1 °C/100 m) occur under the double influence of very high temperatures at the low logger and convective clouds that develop on the ridges of the Jura and help to prevent temperatures from rising as high as they would with clear skies. This effect does not occur during tn because there are no convective clouds at night.

Figure 10: Scatterplot IM (Frequency [% / 100] x Intensity of inversions [°C]) vs Altitudinal Temperature Lapse rate for (A) tn and (B) tx

4.4 Influence of atmospheric conditions on the frequency and intensity of inversions

The occurrence, persistence, and destruction of inversions are determined by climatic conditions (Anquetin et al., 1998; Mernild and Liston, 2009; Bailey et al. 2011). A large number of atmospheric factors play a role in the formation and destruction of inversions (Lareau et al., 2013; Wolf et al., 2016; Vitasse et al., 2017). The diurnal amplitude of temperature was chosen as a proxy for atmospheric conditions. Indeed, west advections accompanied by cloudiness, wind, and frequent precipitation are not conducive to the installation of inversions and destroy them when they do form. On the other hand, calm and cloudless anticyclonic weather is conducive to the formation of inversions during the night because long-wavelength night radiation cools the ground surface. Since the temperature observed at a weather station depends on both radiative and advective influences, diurnal amplitude of temperature is a good integrator of these atmospheric conditions. This choice proved to be judicious because it highlighted the strong relationships that link diurnal amplitude of temperature to inversion frequencies and intensities. It has thus been shown that, when the daily temperature amplitude is low, the average frequency, intensity, and duration of inversions are low too.

However, these results should not mask several limitations with the choice of the diurnal temperature amplitude as an indicator. First of all, temperature amplitudes are a highly simplified reflection of atmospheric conditions. For example, the passage of a front during the day induces an artificially reduced amplitude: the clear morning sky may be replaced by total cloud cover in the afternoon and vice-versa. Thus, the three characters of inversions are not related to mesoscale atmospheric conditions at the time they occur. Despite these limitations, the R^2s resulting from the correlation of temperature amplitude with frequency, intensity, and duration of inversions are high. We can conclude that they reflect the great stability of the weather during the day. If this were the case, it would validate the method; but this point will have to be confirmed.

4.5 Local inversions, regional inversions

There are no simple criteria for distinguishing between different types of inversion. The inversions that concern us in the current work are related to the climatology of topographic hollows where several processes come into play: radiative cooling as everywhere when conditions are favorable and accumulation of cold air from the slopes. Loggers in the upper position are subject to radiative cooling as are lower loggers, but the boundary layer is thinner due to the sliding of cold air downslope. As a result, they are more frequently exposed to the advection of mild air than their lower counterparts. These different processes concern local inversions but not regional inversions because of the greater distances (60 km) and altitudinal amplitude (900 m) separating the paired loggers. Under these conditions, it can only be a question of subsidence inversions: the high parts of the Jura Mountains of France are under the influence of air heated by dry adiabatic compression inside hot high pressure zones while the plain remains cold, with fog or low stratus. These cases are rare since they occur in only 14% of instances in the morning and 4.5% in the afternoon but they may persist for long sequences (5 days or more = 6.1% of inversion sequences) with an average intensity comparable to that of local inversions (2.2 °C).

5 Conclusion

Inversions in the Jura Mountains of France were studied at local and regional scales using respectively 12 and 4 pairs of loggers under forest cover. Comparison with five paired UFC (under forest canopy) and OS (open sites) MF stations confirmed that the inversion frequency values are similar in both contexts. Specific differences have appeared, but they are due to local or temporary particularities that cannot call into question the common characteristics highlighted. The only recurrent difference concerns the intensity of inversions, which is greater in open sites than under forest cover because of the radically different radiation conditions between the two settings. It can be concluded that the results of our study of UFC inversions accurately reproduce the strong trends in the characteristics of open-site inversions.

Local inversions form on more than one day in two in the mornings and one day in five in the afternoons; regional inversions are much less frequent. The intensity is low, both for tn and tx (average 1.8 °C). Even the maximum (15.1 °C) is low compared to that observed by Vitasse et al. (2017) in La Brevine valley near our study area (28 °C). Short inversions (less than a day) are very frequent in the morning (32%) but rare in the afternoon (2%). Inversion sequences of at least one day concern about 15% of the observation period, while persistent inversions of at least three days are relatively rare (totaling 23% of the sequences). Some sequences can be very long-lasting: the maximum is 22 days but two loggers have recorded sequences of more than 20 days' duration. Regional inversions were studied using 4 pairings with an average altitudinal amplitude of 930 m. Their frequency and duration have much lower values while their intensity is comparable. The maximum duration of regional inversions sequences is 6 days.

The three characters (frequency, intensity, and duration) contrast local inversions during tn and the cold seasons (high values) with regional inversions during tx and spring and summer (low values) (Figure 11). However, the relationships between these three elements (local/regional, tn/tx, winter/summer) are not straightforward because regional intensities are higher than local intensities, especially during tx. Moreover, the statistical relationships between them are not always marked.

Figure 11: Synthetic representation of inversion characters

The function, $gradient = f(FI)$, where F is the frequency (expressed from 0 to 1) and I is the intensity of the inversions, highlights the relationship between the altitudinal gradient and the product of two of the inversion characters. The higher ATLR at tn than at tx is largely due to inversions that are more frequent and intense in the morning than in the afternoon, but not only that. Other factors explain this distinctive behavior of ATLRs according to time of day. Further research was not undertaken to try to detect them, as that was not the purpose of this study. But other studies comparable to this one, covering a much larger number of open site logger pairs and over a longer period of time, will need to be conducted to confirm (or invalidate) our results for sites under forest cover.

The influence of atmospheric conditions on the occurrence and characteristics of inversions is fundamental. We have shown this by establishing the relationship between the diurnal thermal amplitude and the frequency, intensity, and duration of inversions. Despite methodological limitations, the results undoubtedly show the close dependence between inversion characteristics and atmospheric conditions. However, there is room for improvement. Atmospheric conditions, rather than being perceived through the diurnal amplitudes of temperatures alone, could be understood by means of climate simulations that provide information on most of the variables that play a role in inversions: radiation, wind, and precipitation.

The results of this study cannot readily be generalized to areas larger than the Jura Mountains of France which, by the nature of its topography, is very different from the surrounding regions whether nearby or further afield. In order to provide more general results, this analysis will be reproduced throughout France using the stations in the Météo-France network.

Finally, the analysis of inversion characteristics has not been related here to the spatial situation and topographical context of the stations. The particularly high frequency and intensity of inversions in the three most easterly locations supports the idea that the continental nature of the climate, which is more pronounced there than anywhere else, has a strong influence on inversions. The aspect and depth of the valleys probably also play a role. These points will be studied in another contribution.

Acknowledgments We thank Météo-France for providing data free-of-charge, the "Parc Naturel Régional du Haut-Jura" and the "Conseil Régional Franche-Comté" which largely financed this study as part of the "Haut-Jura: l'énergie du territoire" LEADER programme, the "Long-term ecological research site Jurassian Arc" (http://zaaj.univ-fcomte.fr/?lang=en) for purchasing some of the loggers and the local mayors and private landowners who allowed us to set up the loggers in forest plots belonging to them.

References

Anquetin S, Guilbaud C, Chollet JP (1998) The formation and destruction of inversion layers within a deep valley. J Appl Meteor 37:1547-1560

Antonioli S (2016) Lapse rate inversions in the Po valley: a 30-year overview. Master "Environmental and Land Planning Engineering", Polytechnico Milano, 97 p

Bailey A, Chase TN, Cassano JJ, Noone D (2011) Changing Temperature Inversion Characteristics in the US Southwest and Relationships to Large-Scale Atmospheric Circulation. J Appl Meteor and Climatol 50(6): 1307-1323

Barry RG (1983) Arctic Ocean Ice and Climate. Perspectives on a Century of Polar Research. Annals of the Ass Amer Geogr, 73(4):485-501

Barry RG (2008) Mountain Weather and Climate. 3rd ed. Cambridge University Press, 506 p

Brümmer B, Schultze M (2015) Analysis of a 7-year low-level temperature inversion data set measured at the 280 m high Hamburg weather mast. Meteorologische Zeitschrift 24(5):481-494

Chemel C, Arduini G, Staquet C, Largeron Y, Legain D, Tzanos D, et al. (2016) Valley heat deficit as a bulk measure of wintertime particulate air pollution in the Arve River Valley. Atmos. Env. 128:208-215

Czarnecka M, Nidzgorska-Lencewicz J (2017) The impact of thermal inversion on the variability of PM10 concentration in winter seasons in Tricity. Environment Protection Engineering 44(2): 157-172. doi: 10.5277/epe170213

Daly C, Conklin DR, Unsworth MH (2010) Local atmospheric decoupling in complex topography alters climate change impacts. Int J Climatol 30(22):1857-1864; doi: 10.1002/joc.2007

Dobrowski SZ (2011) A climatic basis for microrefugia: the influence of terrain on climate. Global Change Biology 17:1022-1035

Dorninger M, Whiteman CD, Bica B, Eisenbach S, Pospichal B, Steinacker R (2011) Meteorological events affecting cold-air pools in a small basin. Journal Appl Meteorol Climatol 50:2223-2234

Dupont JC, Haeffelin M, Stolaki S, Elias T (2016) Analysis of Dynamical and Thermal Processes Driving Fog and Quasi-Fog Life Cycles Using the 2010–2013 ParisFog Dataset. Pure Appl. Geophys. 173:1337-1358; doi 10.1007/s00024-015-1159-x

El Melki T (2007) Inversions thermiques et concentrations de polluants atmosphériques dans la basse troposphère de Tunis. Climatologie. doi.org/10.4267/climatologie.773

Erpicum M (2004) Discrimination des effets radiatifs et des effets advectifs à partir des observations de températures du réseau météo-routier de Wallonie. Norois. doi : 10.4000/norois.1184

Fallot JM (2012) Influence de la topographie et des accumulations d'air froid sur les températures moyennes mensuelles et annuelles en Suisse. In Bigot S. et Rome S. (eds.). 25ème colloque de l'Association Internationale de Climatologie (AIC): 273-278.

Fernando HJS, Verhoef B, Di Sabatino S, Leo LS, Park S (2013) The Phoenix Evening Transition Flow Experiment (TRANSFLEX). Boundary-Layer Meteor. 147: 443-468, doi:10.1007/s10546-012-9795-5

Foster C. S., Crosman E. T., Horel J. D. (2017) Simulations of a Cold-Air Pool in Utah's Salt Lake Valley: Sensitivity to Land Use and Snow Cover. Boundary-Layer Meteor 164:63-87

Gardner A.S., Sharp M.J., Koerner R.M., Labine C., Boon S., Marshall S.J., Burgess D.O., Lewis D. (2009) Near-surface temperature lapse rates over Arctic glaciers and their implications for temperature downscaling. Journal of Climate 22(16):4281-4298. doi:10.1175/2009JCLI2845.1

Gaudio N., Gendre X., Saudreau M., Seigner V., Balandier P. (2017) Impact of tree canopy on thermal and radiative microclimates in a mixed temperate forest: A new statistical method to analyse hourly temporal dynamics. Agr Forest Meteorol 237-238:71-79

Guédjé FK, Houéto VVA, Houngninnou E (2017) Features of the low–level temperature inversions at Abidjan upper-air station (Ivory Coast). Journal of materials and Envir Sciences 8(1):264-272.

Hannah L, Flint L, Syphard AD, Moritz MA, Buckley LB, McCullough IM (2014) Fine-grain modeling of species' response to climate change: holdouts, stepping-stones, and microrefugia. Trends in Ecology & Evolution 29:390-397.

Hosler C (1961) Low-level inversion frequency in the contiguous United States., Monthly Weather Review 89:319-339

Ji D, Wang Y, Wang L, Chen L, Hu B, Tang G, Xin J, Song T, Wen T, Sun Y, Pan Y, Liu Z (2012) Analysis of heavy pollution episodes in selected cities of northern China. Atmos. Environ. 50:338–348. doi:10.1016/j.atmosenv.2011.11.053

Joly D (2015) Etude comparative de la température en forêt et en espace ouvert dans le parc Naturel Régional du Haut-Jura. Climatologie 11. http://lodel.irevues.inist.fr/climatologie/index.php?id=562

Joly D, Berger A, Buoncristiani JF, Champagne O, Pergaud J, Richard Y, Soare P, Pohl B (2018) Geomatic downscaling of temperatures in the Mont-Blanc massif. Int J Climatol 38(4):1846-1863. doi: 10.1002/joc.5300

Joly D, Gillet F (2017) Interpolation of temperatures under forest cover on a regional scale in the French Jura Mountains. Int J Climatol doi:10.1002/joc.5029

Kadygrov EN, Khaikin MN, Miller EA, Shaposhnikov A, Troitsky AV (2005) Advanced atmospheric boundary layer temperature profiling with MTP-5HE microwave system. In: WMO Technical

conference on Meteorological and Environmental Instruments and Methods of Observation (Teco-2005) Proceedings, Bucharest, Romania, pp 22-26

Kahl JD (1990) Characteristic of the low-level temperature inversion along the Alaska Arctic Coast. Int J Climatol 10:537-548

Karlsson IM (2000) Nocturnal air temperature variations between forest and open areas. J Appl Meteorol 39:851-862

Kiefer MT, Zhong S (2015) The role of forest cover and valley geometry in cold-air pool evolution. J Geophys Res Atmos 120:8693-8711

Kirchner M, Faus-Kessler T, Jakobi G, Leuchner M, Ries L, Scheel HE, Suppan P (2013) Altitudinal temperature lapse rates in an Alpine valley: Trends and the influence of season and weather patterns. Int J Climatol 33(3):539-555. doi:10.1002/joc.3444

Kukkonen J, et al. (2005) Analysis and evaluation of selected local-scale PM air pollution episodes in four European cities: Helsinki, London, Milan and Oslo. Atmos Environ 39(15):2759-2773. doi:10.1016/j.atmosenv.2004.09.090

Lareau NP, Crosman E, Whiteman CD, Horel JD, Hoch SW, Brown WO, Horst TW (2013) The persistent cold-air pool study Bull. Am Meteorol Soc 94(1):51-63

Largeron Y, Staquet C (2016) Persistent inversion dynamics and wintertime PM10 air pollution in Alpine valleys. Atmospheric Environment 135: 92-108. doi.org/10.1016/j.atmosenv.2016.03.045

Li X, Wang L, Chen D, Yang K, Xue B, Sun L (2013) Near-surface air temperature lapse rates in mainland China during 1962–2011. Journal of Geophys Research: Atmospheres 118(14):7505-7515. doi http://doi. org/10.1002/jgrd.50553

Mahrt L, Heald R (2015) Common Marginal Cold Pools. J Appl Meteorol and Climatol 4 (2):339-351

Mahrt L, Richardson S, Seaman N, Stauffer D (2010) Non-stationary drainage flows and motions in the cold pool. Tellus 62:698-705. doi:https://doi.org/10.1111/j.1600-0870.2010.00473.x

Marvin CF, (1914) Air drainage explained. Monthly Weather Review 10:583-585

Mernild SH, Liston G (2009) The Influence of Air Temperature Inversions on Snowmelt and Glacier Mass Balance Simulations, Ammassalik Island, Southeast Greenland. J Appl Meteorol and Climatol 49(1). doi 10.1175/2009JAMC2065.1

Milionis AE, Davies TD (2008) A comparison of temperature inversion statistics at a coastal and a non-coastal location influenced by the same synoptic regime. Theor Appl Climatol 94:225–239

Mirocha JD, Branko K (2010) Large-eddy simulation study of the influence of subsidence on the stably stratified atmospheric boundary layer. Boundary-Layer Meteorol 134(1):1-21. DOI 10.1007/s10546-009-9449-4

Mo R, Joe P, Isaac GA, Gultepe I, Rassemusen R, Milbrandt J, Mctaggart-Cowan R, Mailhot J, Brugman M, Smith T, Scott B (2014) Mid-Mountain Clouds at Whistler During the Vancouver 2010 Winter Olympics and Paralympics. Pure Appl. Geophys 171:157-183 201. doi 10.1007/s00024-012-0540-2

Nigrelli G, Fratianni S, Zampollo A, Turconi L, Chiarle M (2017) - The altitudinal temperature lapse rates applied to high elevation rockfalls studies in the Western European Alps. Theor Applied Climatol Online First. doi: 10.1007/s00704-017-2066-0

Oke TR (1987) Boundary Layer Climates. 2nd ed. Routledge, 435 p.

Pagès M, Pepin N, Miróa JR (2017. Measurement and modelling of temperature cold pools in the Cerdanya valley (Pyrenees), Spain. Meteorol applications 24:290–302

Papadopoulos KH, Helmis CG (1999) Evening and morning transition of katabatic flows. Bound-Layer Meteor 92:195-227. doi.org/10.1023/A:1002070526425

Patsiou TS, Conti E, Theodoridis S, Randin CF (2017) The contribution of cold air pooling to the distribution of a rare and endemic plant of the Alps. Plant Ecology & Diversity 10(1):29-42

Pepin NC, Duane WA (2007) Comparison of surface and free-air temperature variability and trends at radiosonde sites and nearby high elevation surface stations. Int J Climol 27(11):1519-1529. doi: 10.1002/joc.1541

Pepin NC, Norris JR (2005) An examination of the differences between surface and free-air temperature trend at high-elevation sites: Relationships with cloud cover, snow cover, and wind. J Geophy Research 110: D24112. doi: 10.1029/2005JD006150

Paci A, Staquet C, et al. (2015) The Passy-2015 field experiment: an overview of the campaign and preliminary results. Proc. of the 33rd International Conference on Alpine Meteorology, Innsbruck, Austria (2015)

Price J, Vosper S, Brown A, Ross A, Clark P, Davies F, Horlacher V, Claxton B, McGregor J, Hoare J, et al., (2011) COLPEX: field and numerical studies over a region of small hills. Bull. Am. Meteorol Soc 9(12):1636-1650

Prömmel K, Geyer B, Jones JM, Widmann M (2010) Evaluation of the skill and added value of a reanalysis-driven regional simulation for Alpine temperature. Int J Climol 30:760–773. doi: 10.1002/joc.1916

Rolland C (2003) Spatial and seasonal variations of air temperature lapse rates in Alpine regions. J Climate 16(7):1032-1046. doi: 10.1175/1520-0442(2003)016<1032:SASVOA>2.0.CO;2.

Shimokawabe A, Yamaura Y, Akasaka T, Sato T, Shida Y, Yamanaka S, Nakamura F (2015) The distribution of cool spots as microrefugia in a mountainous area. PLoS ONE 10. doi: e0135732. https://doi.org/10.1371/journal.pone.0135732

Sotiropoulou G, Tjernström MG, Sedlar J, Achtert P, Brooks BJ, Brooks IM, Persson OG, Prytherch J, Salisbury DJ, Shupe MD, Johnston PE, Wolfe D (2016) Atmospheric Conditions during the Arctic Clouds in Summer Experiment (ACSE): Contrasting Open Water and Sea Ice Surfaces during Melt and Freeze-Up Seasons. Amer Meteorol Soc 29:8721-8744. doi: 10.1175/JCLI-D-16-0211.1

Schuster C, Kirchner M, Jakobi G (2014) Frequency of inversions affects senescence phenology of Acer pseudoplatanus and Fagus sylvatica. Int J Biometeorol. 58(4):485-498. doi.org/10.1007/s00484-013-0709-0

Streten NA., Ishikawa N, Wendler G, (1974) Some observations of the local wind regime on an Alaskan Arctic Glacier. Arch Meteor Geophys Bioklimatol Ser. B 22:337–350

Vitasse Y, KleinJames G, Kirchner JW, Rebetez M (2017) Intensity, frequency and spatial configuration of winter temperature inversions in the closed La Brevine valley, Switzerland. Theor Appl Climatol 130(3-4):1073-1083

Whiteman CD, Bian X, Zhong S, (1999) Wintertime Evolution of the Temperature Inversion in the Colorado Plateau Basin. J Appl Meteorol 38:1103-1117

Whiteman CD, Zhong S, Shaw WJ, Hubbe JM, Bian X, Mittelstadt J (2001) Cold pools in the Columbia basin. Weather Forecasting 16:432-447

Wolf T, Esau I, Reuder J (2016) Analysis of the vertical temperature structure in the Bergen valley, Norway, and its connection to pollution episodes, and its connection to pollution episodes. J Geophys Research - Atmospheres 119:10645–10662

Zhang Z, Gong D, Mao R, Kimd SJ, Xub J, Zhao X, Ma Z (2017) Cause and predictability for the severe haze pollution in downtown Beijing in November–December 2015. Science of The Total Environment 592:627-638. https://doi.org/10.1016/j.scitotenv.2017.03.009

Fig1

Click here to download Figure fig1.tif

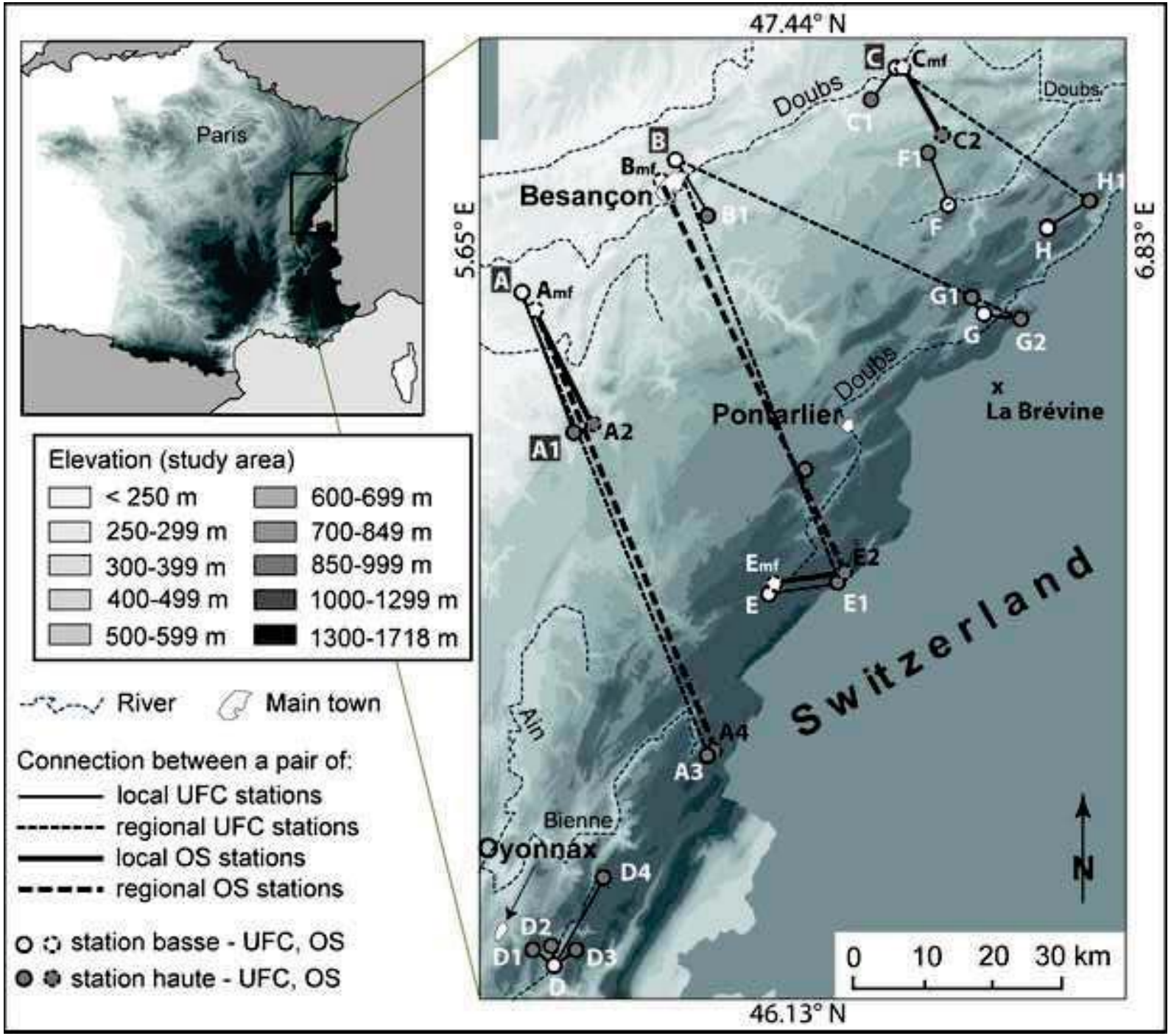

Fig2

Click here to download Figure fig2.tif

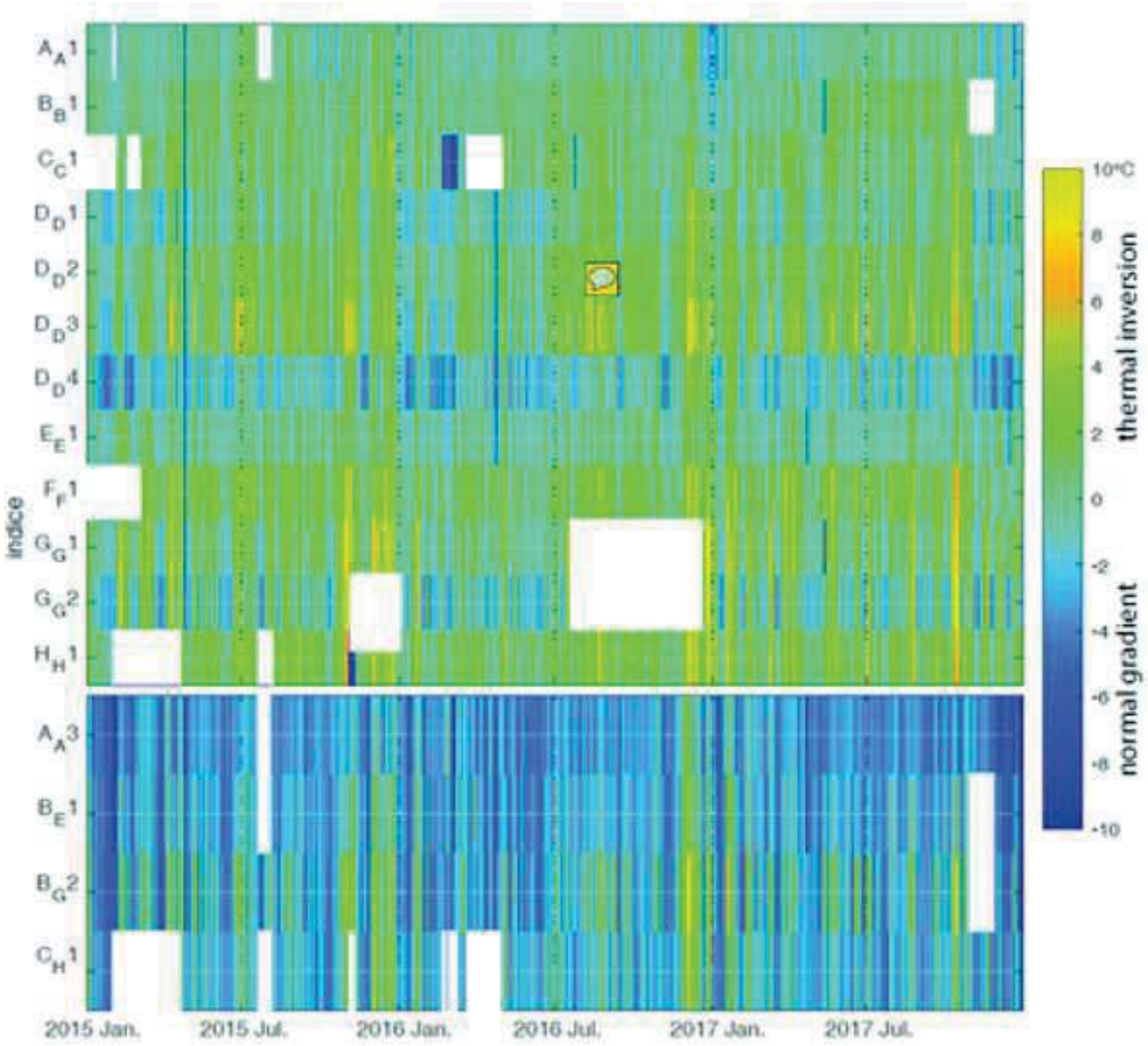

Fig3

Click here to download Figure Fig3.tif

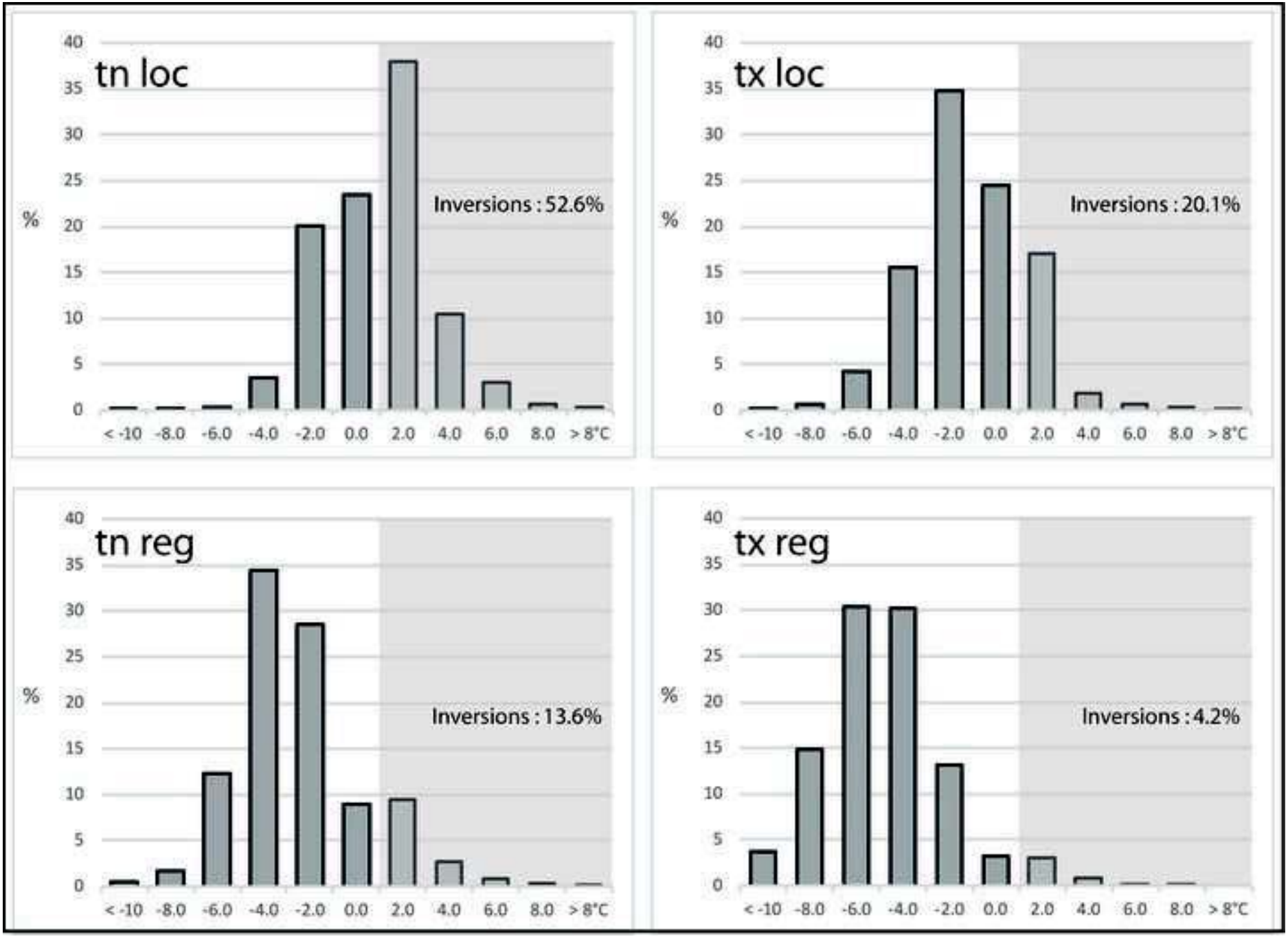

Fig4

Click here to download Figure fig4.tif

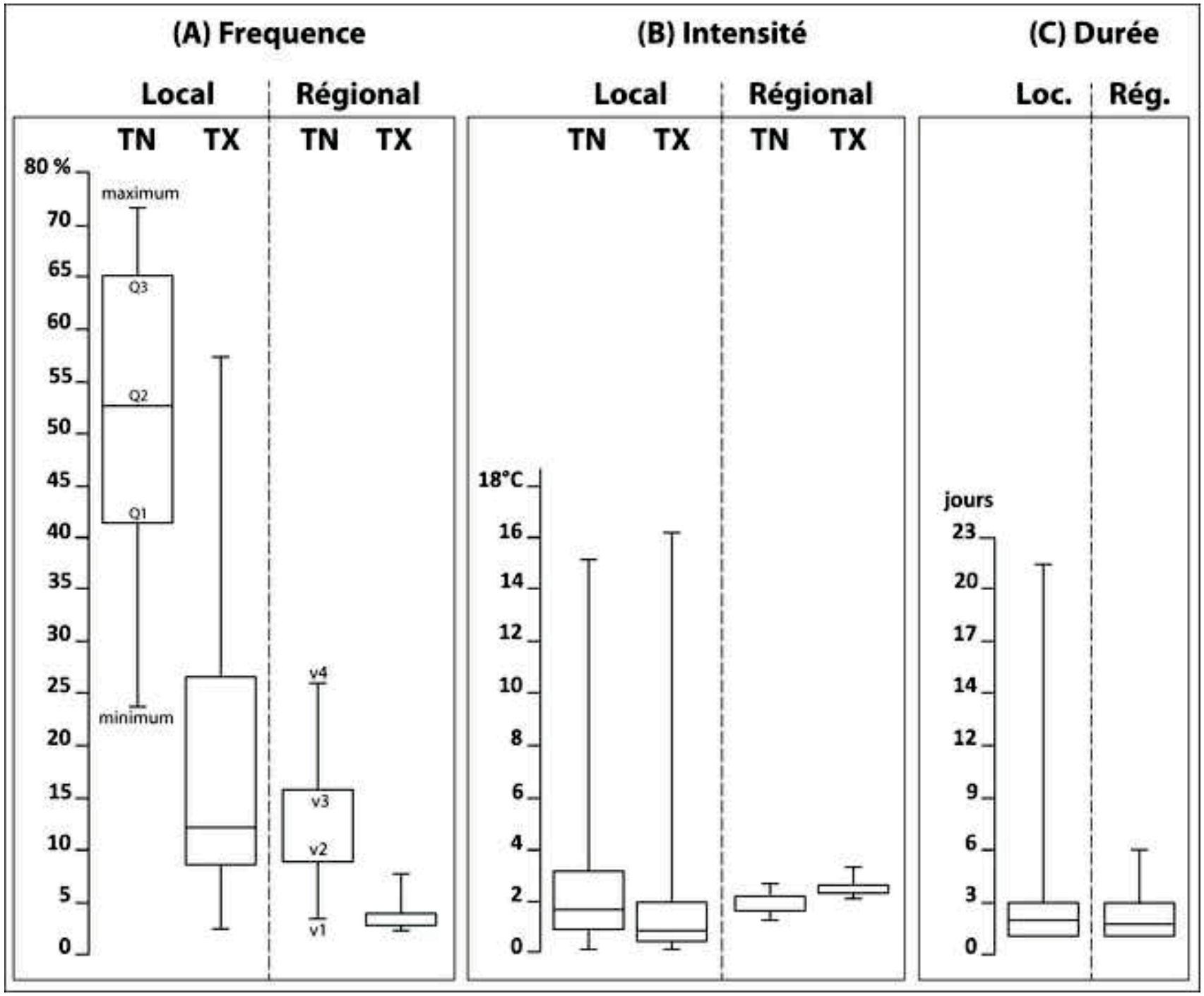

Fig5

Click here to download Figure fig5.tif

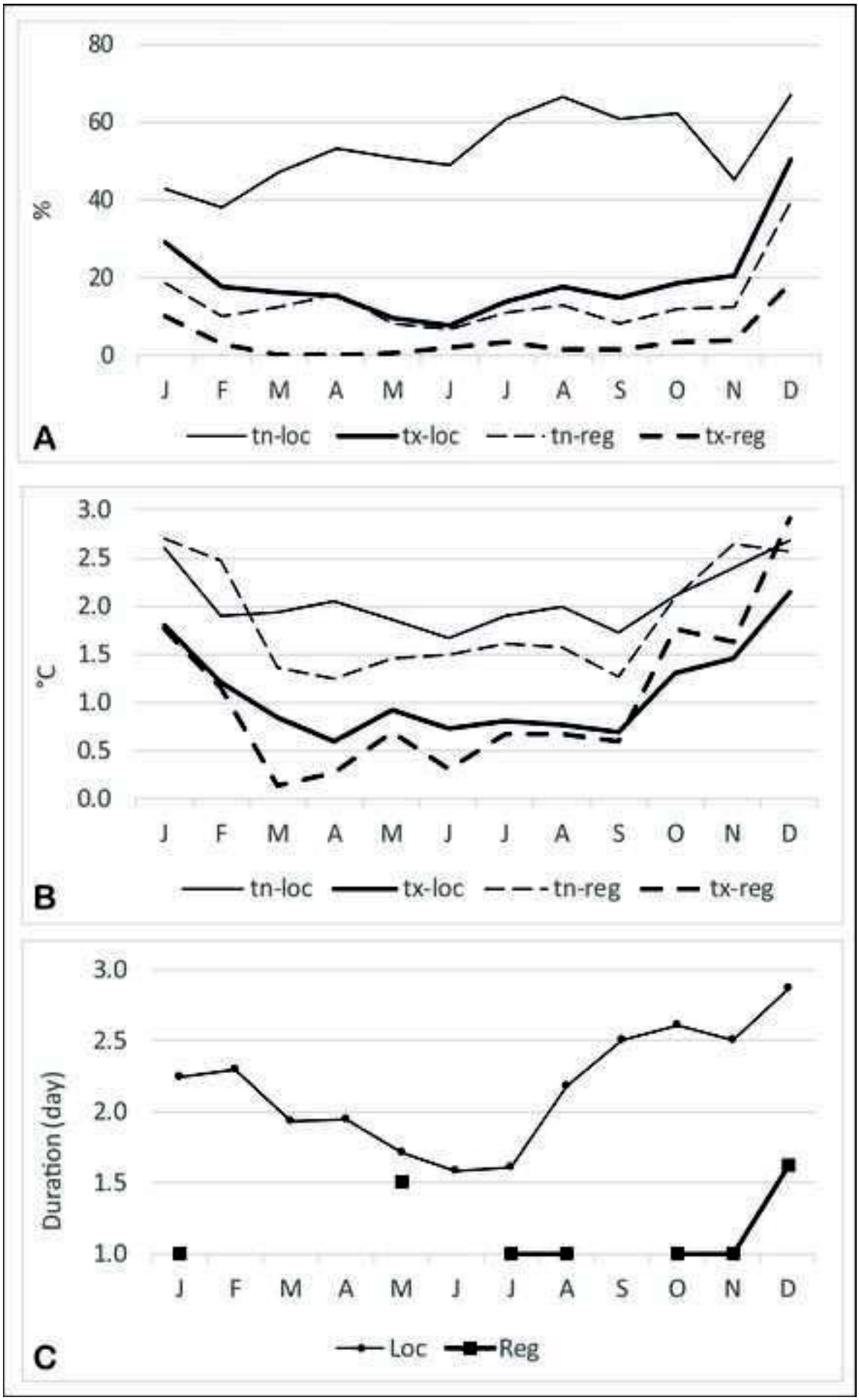

Fig6

Click here to download Figure fig6.tif

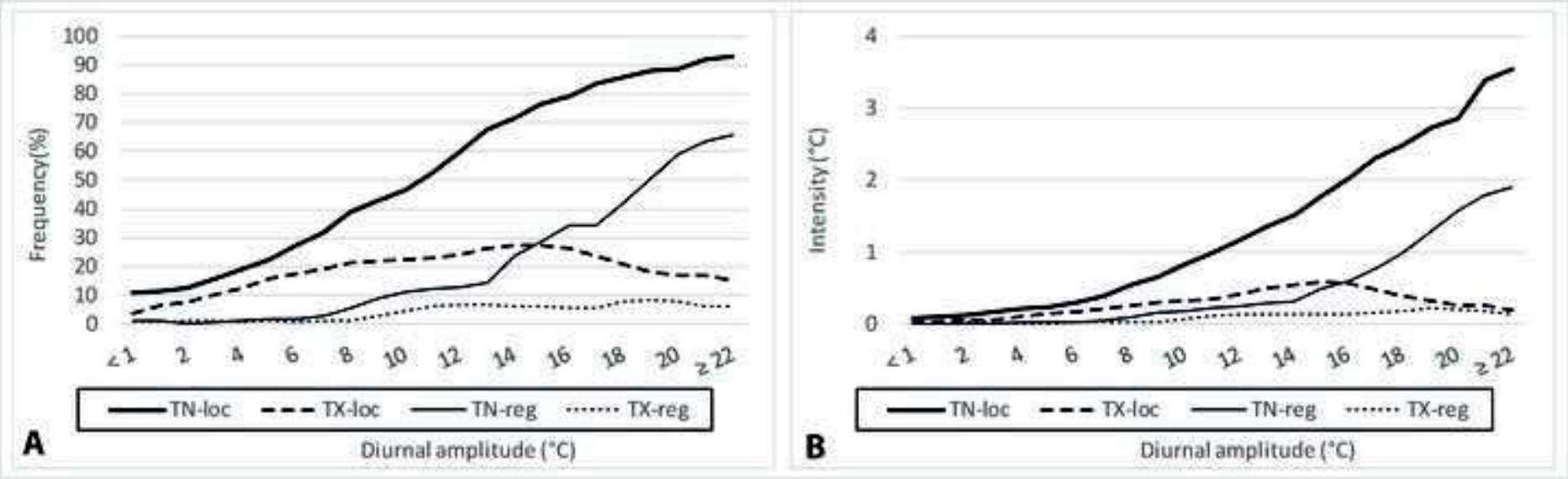

Fig7

Click here to download Figure fig7.tif

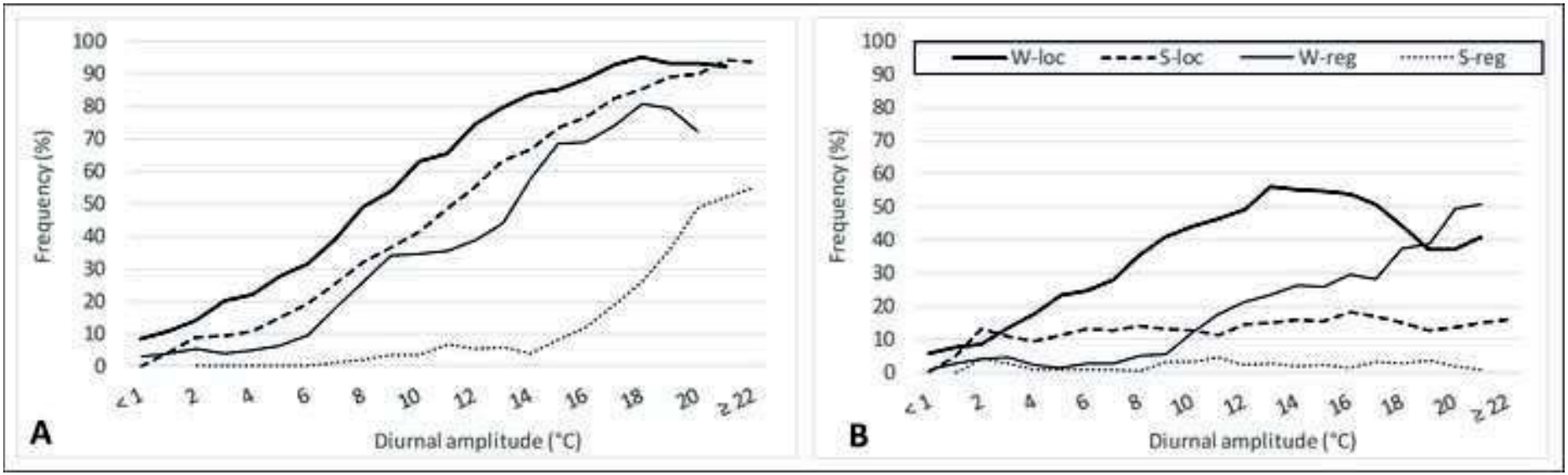

Fig8

Click here to download Figure fig8.tif

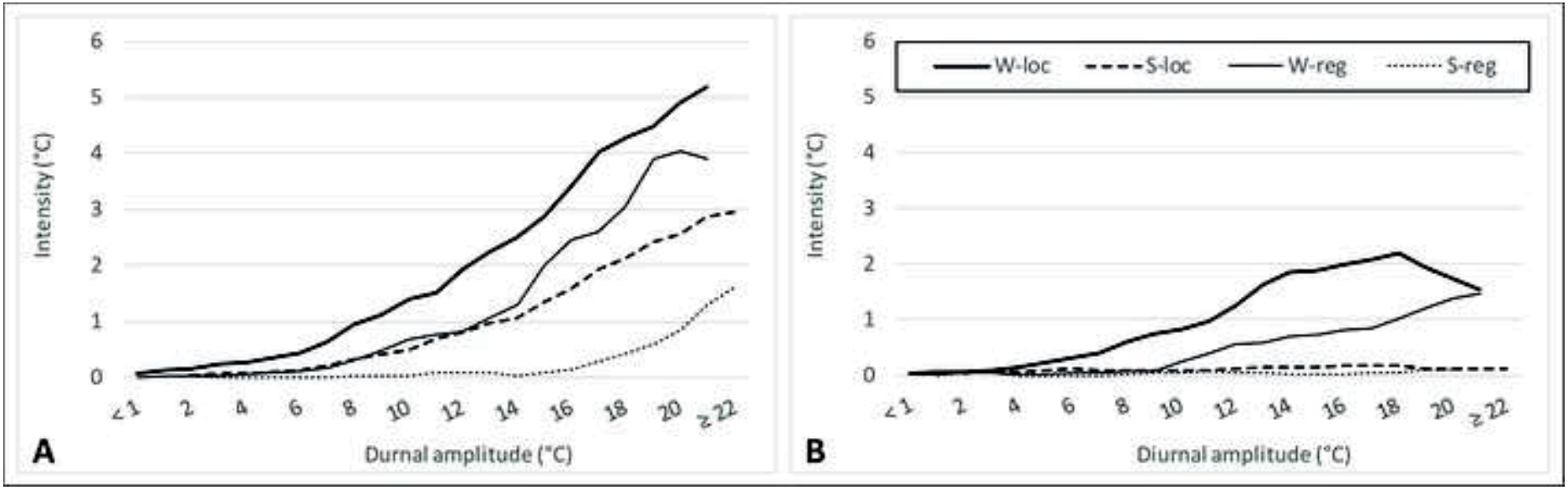

Fig9

Click here to download Figure fig9.tif

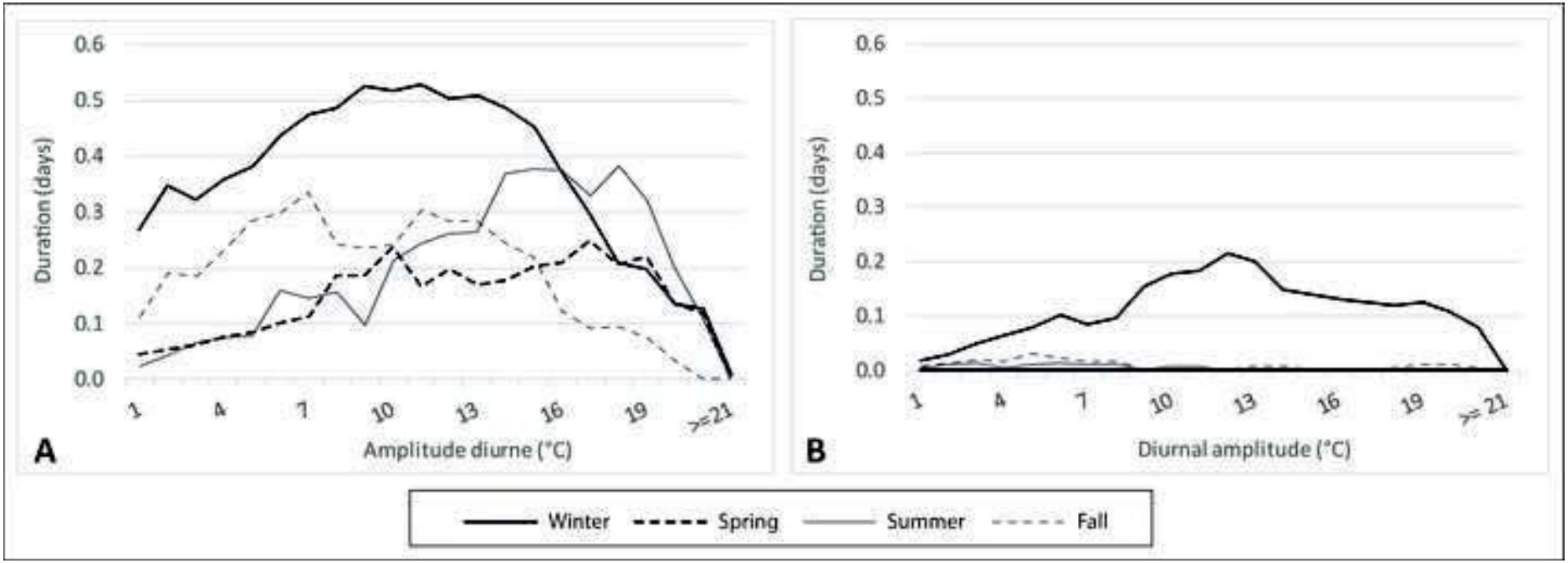

Fig10

Click here to download Figure fig10.tif

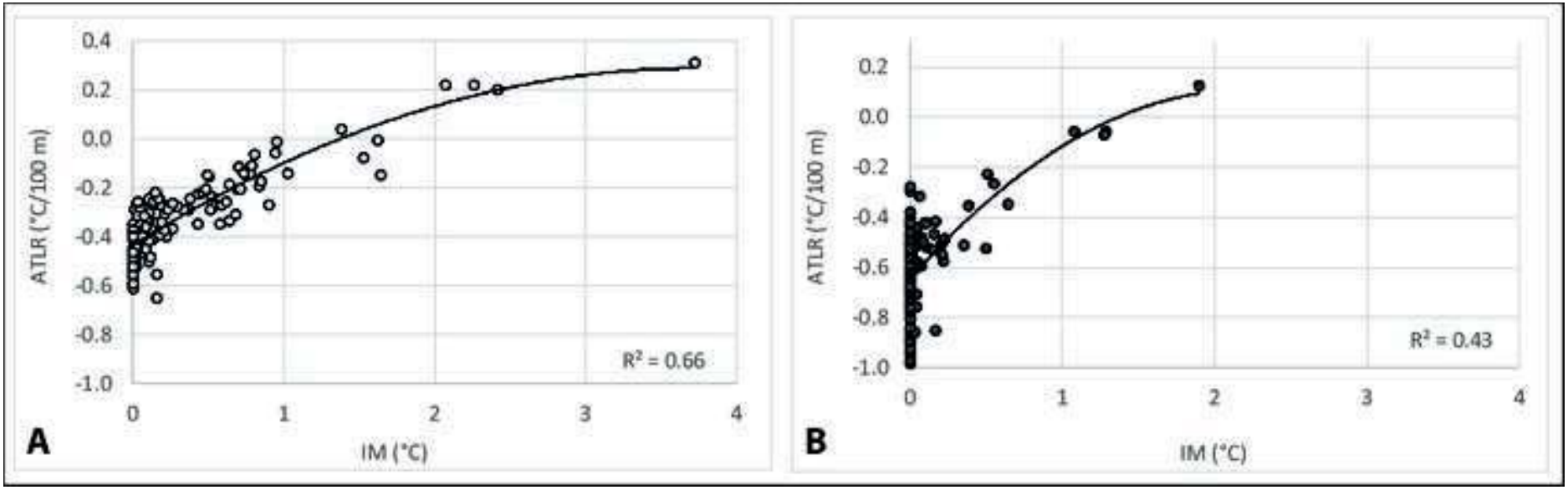

Fig11

Click here to download Figure fig11.tif